Int. J. Electrochem. Sci., 17 **(2022)** Article Number: 220851, doi: 10.20964/2022.08.51

International Journal of
ELECTROCHEMICAL
SCIENCE
www.electrochemsci.org

Short Communication

Effect of Different Sealing Treatments of Oxide Films on Corrosion Resistance of Anodized ZL101A Aluminum Alloy in Simulated Marine Atmospheric Environment

Huarui Zhao[1,*], *Xinghua Chen*[1], *Xinjieyuan*[1], *Lilizhou*[1], *Xinliang Wang*[2]

[1] Xinxiang Vocational and Technical College, Xinxiang 453000, China;
[2] Xinxiang College, Xinxiang 453000, China
[*]E-mail: Zhao_edu453@126.com

Received: 17 April 2022 / *Accepted:* 9 June 2022 / *Published:* 4 July 2022

In order to further improve the corrosion resistance of ZL101A aluminum alloy, which is commonly used in automobiles, an anodic oxide film was prepared on the surface of ZL101A aluminum alloy by conventional anodizing process, followed by sealing treatment in a mixed solution containing nickel salt and cerium salt. The protection effect of the conventional anodic oxide film and sealed anodic oxide films on ZL101A aluminum alloy in simulated marine atmospheric environment were investigated. The results show that after boiling water sealing, nickel salt sealing and synergistic sealing with nickel salt and cerium salt, the surface composition and phase of conventional anodic oxide film change. The reaction products generated during sealing fill the defects of anodic oxide film due to volume expansion and deposition effect resulting in the improvement of the corrosion resistance. After synergistic sealing with nickel salt and cerium salt, hydrated alumina, hydroxide precipitate and cerium hydroxide precipitate are simultaneously generated to play multiple sealing functions. Therefore, the anodic oxide film after synergistic sealing with nickel salt and cerium salt possesses the best corrosion resistance, and it plays a good protective role, allowing ZL101A aluminum alloy to meet the high requirements of application in simulated marine atmospheric environment.

Keywords: Simulated marine atmospheric environment; Anodic oxide film; Corrosion resistance; ZL101A aluminum alloy; Protection effect

1. INTRODUCTION

ZL101A aluminum alloy has excellent machinability, weldability and casting performance, and it is often employed to manufacture gearbox boxes, volute, valve body and automotive parts [1-3]. ZL101A aluminum alloy has a strong affinity with oxygen, and its surface is easily oxidised forming a layer of amorphous natural oxide film, which has a certain role in corrosion protection. The natural

oxide film, on the other hand, is far too thin to serve as a reliable protective layer. In particular, when in the marine atmospheric environment, the destruction of the natural oxide film on the surface of ZL101A aluminum alloy will be accelerated, due to dry and wet alternation leading to serious corrosion which reduce the reliability of automobile parts.

Therefore, for the purpose of further improving the corrosion resistance of ZL101A aluminum alloy, it is usually anodized and sealed [4-8]. Through anodic oxidation, a dense and porous anodic oxide film is generated on the surface of ZL101A aluminum alloy, and then the pores of anodic oxide film can be filled and blocked via different sealing processes, considerably enhancing the corrosion resistance of anodic oxide film and ensuring that the ZL101A aluminium alloy parts meet the requirements in marine atmospheric environment [9-13]. In recent years, some reports on the anodic oxidation and sealing treatment of ZL101A aluminium alloy have been published, but the majority of them are aimed at the conventional anodic oxidation process and a single-sealing process. It has been discovered that the synergistic sealing treatment of anodic oxide film is of great significance which is expected to realize the superposition of sealing effect of different sealing processes, so as to ensure the durability of anodic oxide film meet the application requirements [14-16]. In this paper, an anodic oxide film was prepared on the surface of ZL101A aluminum alloy by conventional anodizing process, followed by sealing treatment in a mixed solution containing nickel salt and cerium salt. In simulated marine atmospheric environment, the protection effect of conventional anodic oxide film and sealed anodic oxide films on ZL101A aluminum alloy in simulated marine atmospheric environment were investigated.

2. EXPERIMENTAL

2.1 Preparation of different anodic oxide films

ZL101A aluminum alloy plate was cut into samples of 50 mm×30 mm×2 mm which were then polished step by step with 400#, 1000# and 2000# sandpapers. The samples were cleaned with ultrasonic wave in a solution of acetone and anhydride ethanol for 8 min. After that, the samples were immersed into nitric acid solution of 10% volume fraction for activation, before being cleaned with deionized water.

FST-150A power supply was used for anodic oxidation, and the current density was 2 A/dm^2 with constant current mode. ZL101A aluminum alloy sample was used as anode and pure aluminum plate was used as cathode. The composition of the electrolyte is 98% sulphuric acid 100 g/L mixed with oxalic acid 25 g/L. The temperature of the electrolyte was maintained at (20±0.5)℃ using water bath heat. The anodic oxidation time was 50 min, and a conventional anodic oxide film was formed on the surface of ZL101A aluminum alloy sample.

2.2 Sealing treatment of anodic oxide films

The anodized ZL101A aluminum alloy samples were post-treatment via boiling water sealing (BWS), nickel salt sealing (NSS) and synergistic sealing with nickel salt and cerium salt (NSS and

CSS) respectively. Table 1 shows the solution composition and conditions of different sealing processes.

Table 1. Solution composition and conditions of different sealing processes

Different sealing processes	Composition	Conditions
BWS	pure water	100℃, 30 min
NSS	$NiSO_4$ 6 g/L, H_3BO_3 2 g/L CH_3COONa 5 g/L	90℃, 30 min
NSS and CSS	$NiSO_4$ 6 g/L, H_3BO_3 2 g/L CH_3COONa 5 g/L, $Ce(NO_3)_3$ 18 g/L	90℃, 25 min

2.3. Performance testing

The surface composition of different anodic oxide films was analyzed by INCA-300 energy dispersive spectrometer, and the phase of different anodic oxide films was analyzed by D8 Advance X-ray diffractometer combined with Jade software with acceleration voltage 40 kV, current 30 mA and scanning angle range 20°~90°.

Fi-65 type of dry-wet periodic infiltration corrosion tester was used to simulate the marine atmosphere environment, and a mixed solution of 3.5% sodium chloride, 2‰ sodium sulfate and 1‰ magnesium chloride was used as the corrosion medium. The relative humidity in the box was 60%~80%, and the temperature was (40±2)℃. The samples were immersed in the mixed solution for 15 min and then dried for 45 min. Each drying and wetting cycle was 60 min, lasting for 360 cycles in total. After the experiment, the samples were cleaned with deionized water, and then dried with cold air. The corrosion morphology of different anodic oxide films was characterized by XL-30-FeG scanning electron microscope.

A classical three-electrode system was used to test the polarization curves of different anodic oxide films immersed in a mixed solution of 3.5% sodium chloride, 2‰ sodium sulfate and 1‰ magnesium chloride for different time. The samples with anodic oxide film on both sides of the working electrode were exposed to an area of 10 mm×10 mm on the working surface, and the non-working surface was coated with epoxy resin adhesive. Platinum plate was used as auxiliary electrode and saturated calomel electrode was as reference electrode. The polarization curve test potential was ±300 mV relative to the open circuit potential, and the scanning rate was 1 mV/s.

3. RESULT AND DISCUSSION

3.1 Surface composition and phase of different anodic oxide films

Figure 1 shows the surface composition of different anodic oxide films. It can be seen from Figure 1 that the surface composition of the conventional anodic oxide film is Al, O and S elements, of

which the mass fraction of Al element is the highest and the mass fraction of S element is the lowest. After boiling water sealing, nickel salt sealing and synergistic sealing with nickel salt and cerium salt, the surface composition of conventional anodic oxide film is changed. Except for Al, O and S elements, C and Ni elements as well as Ce element are introduced accordingly. During the boiling water sealing, reaction (1) occurs to generate hydrated alumina, and during the reaction, carbides enter the anodic oxide film, resulting in C element in the anodic oxide film. Reactions (1) and (2) occur during the nickel salt sealing, both hydrated alumina and nickel hydroxide precipitation are absorbed on the anodic oxide film with C and Ni elements. Reactions (1), (2) and (3) occur simultaneously during the synergistic sealing with nickel salt and cerium salt, resulting in the formation of hydrated alumina, nickel hydroxide precipitation and cerium hydroxide precipitation with C, Ni and Ce elements [17-20].

$$Al_2O_3 + H_2O \rightarrow 2Al(OH) \quad (1)$$

$$Ni^{2+} + 2H_2O \rightarrow Ni(OH)_2 \downarrow + 2H^+ \quad (2)$$

$$Ce^{3+} + 3OH^- \rightarrow Ce(OH)_3 \downarrow \quad (3)$$

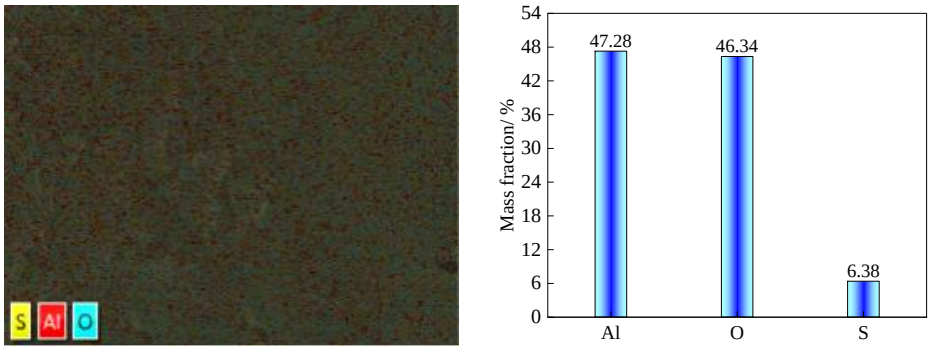

(a) conventional anodic oxide film

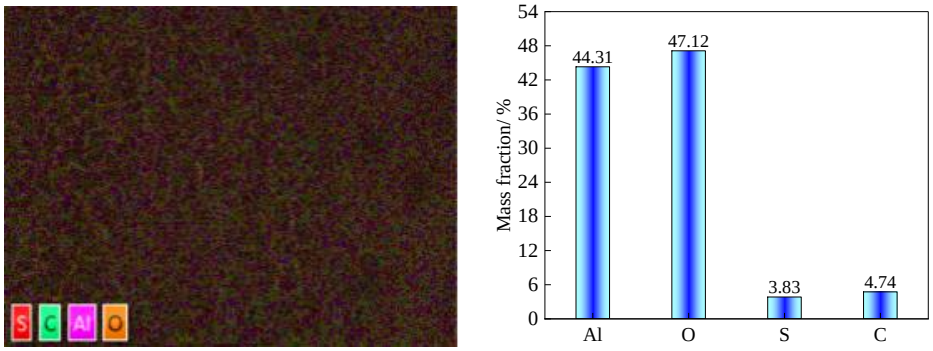

(b) anodic oxide film after BWS

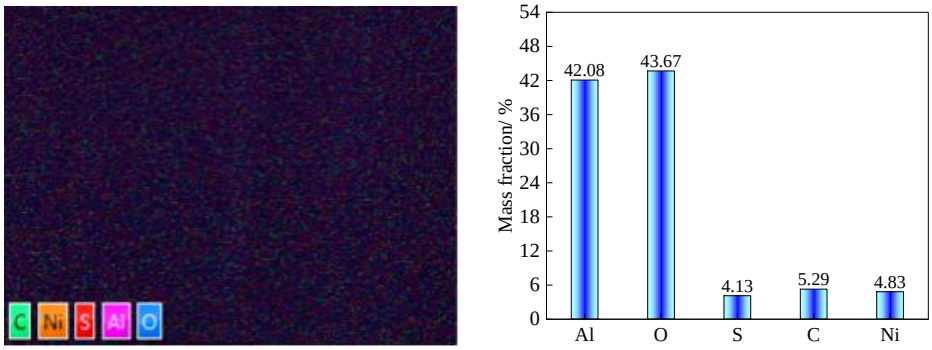

(c) anodic oxide film after NSS

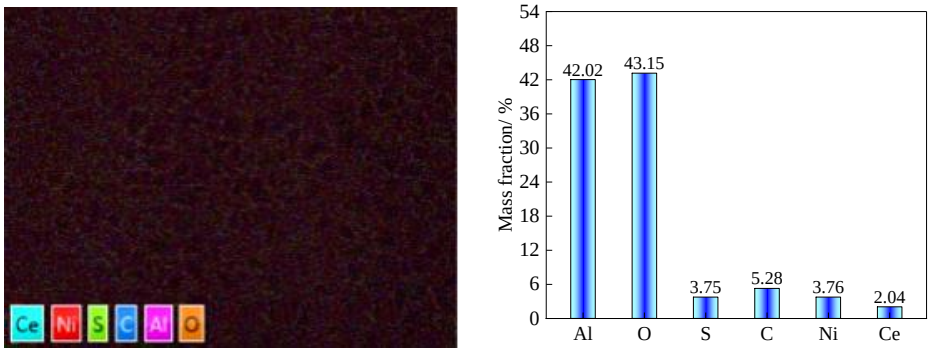

(d) anodic oxide film after NSS and CSS

Figure 1. Surface composition of different anodic oxide films

Figure 2 shows the XRD diffraction spectrum of different anodic oxide films. According to XRD diffraction spectrum analysis, the phase of the anodic oxide film after BWS is unchanged compared with conventional anodic oxide film, which is composed of α-Al_2O_3 and γ-Al_2O_3 phases [21-22]. However, the phase of the anodic oxide film changed after NSS. In addition to α-Al_2O_3 and γ-Al_2O_3 phases, there are also $Ni(OH)_2$ phase. It can be confirmed that nickel hydroxide precipitation is generated and doped in anodic oxide film during nickel salt sealing. However, $Ce(OH)_3$ phase is not found in XRD diffraction spectrum, which may result in lower $Ce(OH)_3$ content doped in the anodic oxide film during synergistic sealing with nickel salt and cerium salt. Other kinds of sealing treatments for aluminum are also reported in some papers, including cerium sealing, cobalt salt sealing and so on [23-25].

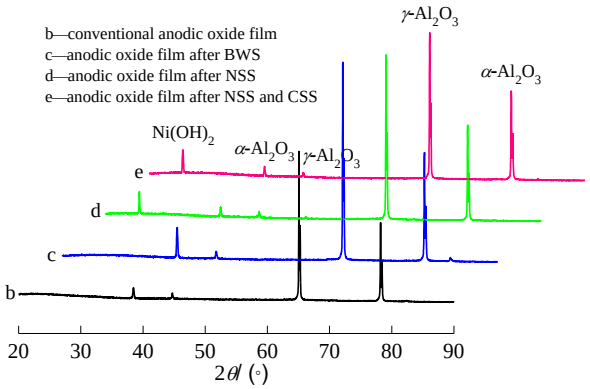

Figure 2. XRD diffraction spectrum of different anodic oxide films

3.2 Protection effect of different anodic oxide films on ZL101A aluminum alloy

3.2.1 Corrosion morphology analysis

Figure 3 shows the corrosion morphology of ZL101A aluminum alloy and different anodic oxide films. As can be seen from Figure 3(a), after 360 cycles of dry and wet alternating experiments in simulated marine atmospheric environment, serious pitting and cracking are found on the surface of ZL101A aluminum alloy to form some fine pits and deep irregular depressions. These pits and depressions spread outwards, forming large areas of corrosion. As can be seen from Figure 3(b)~3(e), after 360 cycles of dry and wet alternating experiments in simulated marine atmosphere, no cracking phenomenon is found in conventional anodic oxide film and sealed anodic oxide films, and the corrosion degree was significantly reduced in contrast to ZL101A aluminum alloy. This is because during sealing treatment, hydrated alumina, nickel hydroxide precipitation and cerium hydroxide precipitation are generated to fill the defects of the anode oxide films that can cut off the corrosive ions from moving inside of anodic oxide film resulting in the improvement of corrosion resistance. Similar sealing mechanism about the precipitation of metal oxides and hydroxides is also reported by some scholars [26-28]. In comparison, the corrosion degree of the anodic oxide film after NSS and CSS is the lightest. The corrosion pits and depressions formed on the surface are shallow and few in number, with the corrosion area being the smallest. It is known that, synergistic sealing with nickel salt and cerium salt can generate hydrate alumina, nickel hydroxide precipitation and cerium hydroxide precipitation simultaneously to better fill the pores and defects of anodic oxide film while improving its compactness, which leads to the best corrosion resistance.

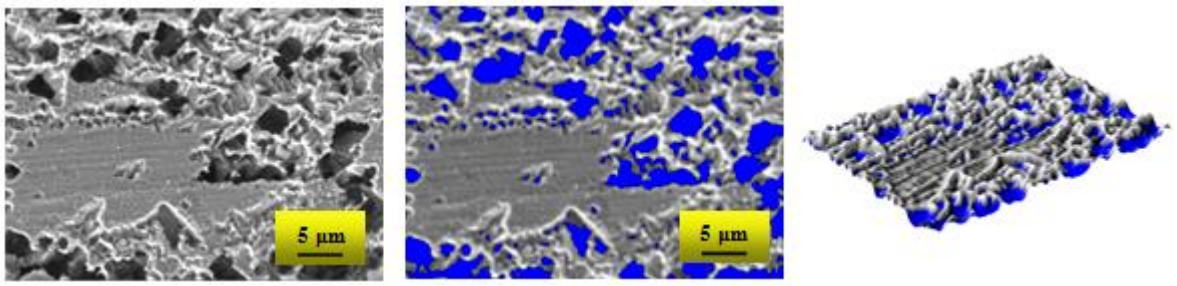

(a) ZL101A aluminum alloy

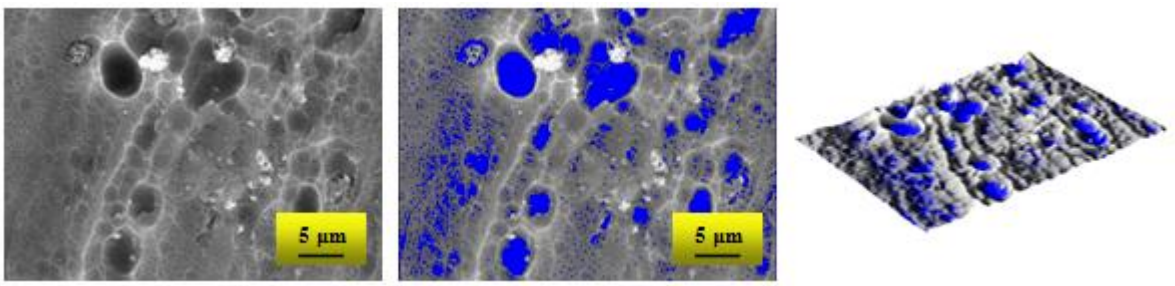

(b) conventional anodic oxide film

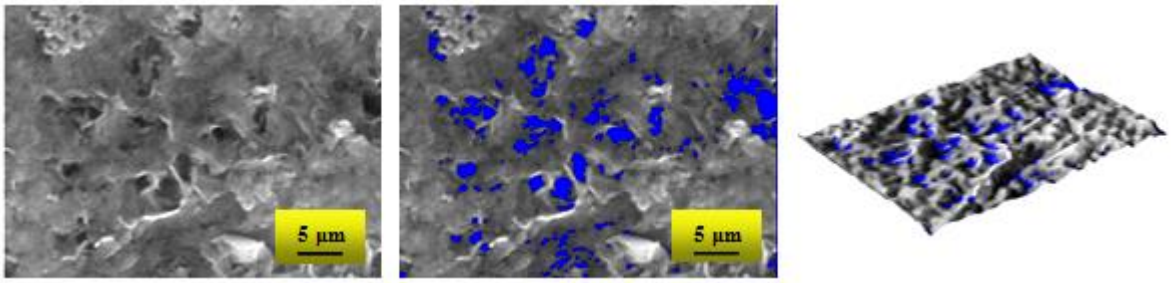

(c) anodic oxide film after BWS

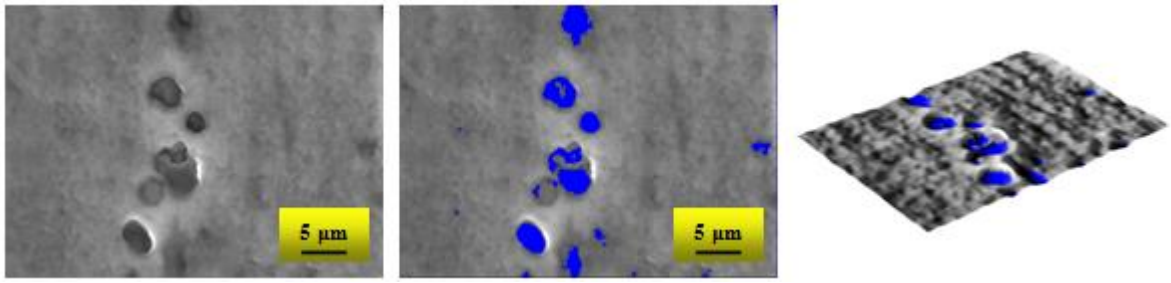

(d) anodic oxide film after NSS

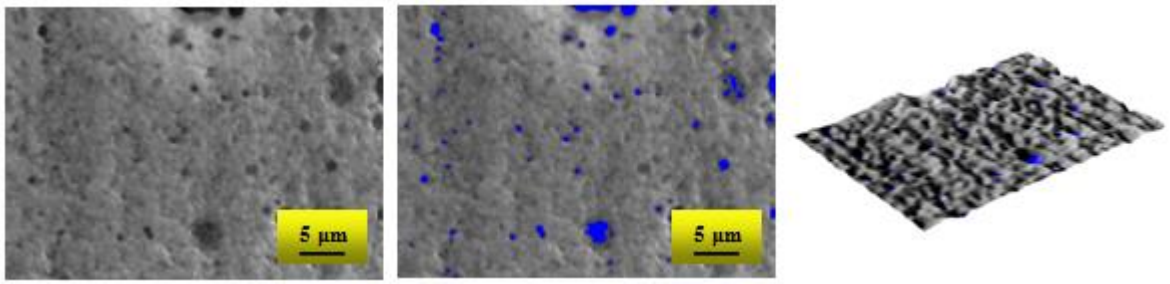

(e) anodic oxide film after NSS and CSS

Figure 3. Corrosion morphology of ZL101A aluminum alloy and different anodic oxide films

3.2.2 Corrosion products analysis

Figure 4 shows the composition of corrosion products on the surface of ZL101A aluminum alloy and different anodic oxide films. As can be observed from Figure 4 that the corrosion products on the surface of ZL101A aluminum alloy contain Al, O, C, Cl, Na and other elements due to NaCl crystals and $AlCl_3$ adsorbed carbon oxides on the surface of ZL101A aluminum alloy. Some scholars also investigate the corrosion products of aluminum and aluminum alloys [29-30]. The corrosion products of conventional anodic oxide film also contain Al, O, C, Cl, Na and other elements, but with lower mass fraction of Cl and Na elements, confirming the corrosion degree of conventional anodic oxide film is reduced compared with ZL101A aluminum alloy. After boiling water sealing, nickel salt sealing and synergistic sealing with nickel salt and cerium salt, the corrosion products on the surface of anodic oxide film are less, and the mass fraction of C, Cl and Na elements is much lower.

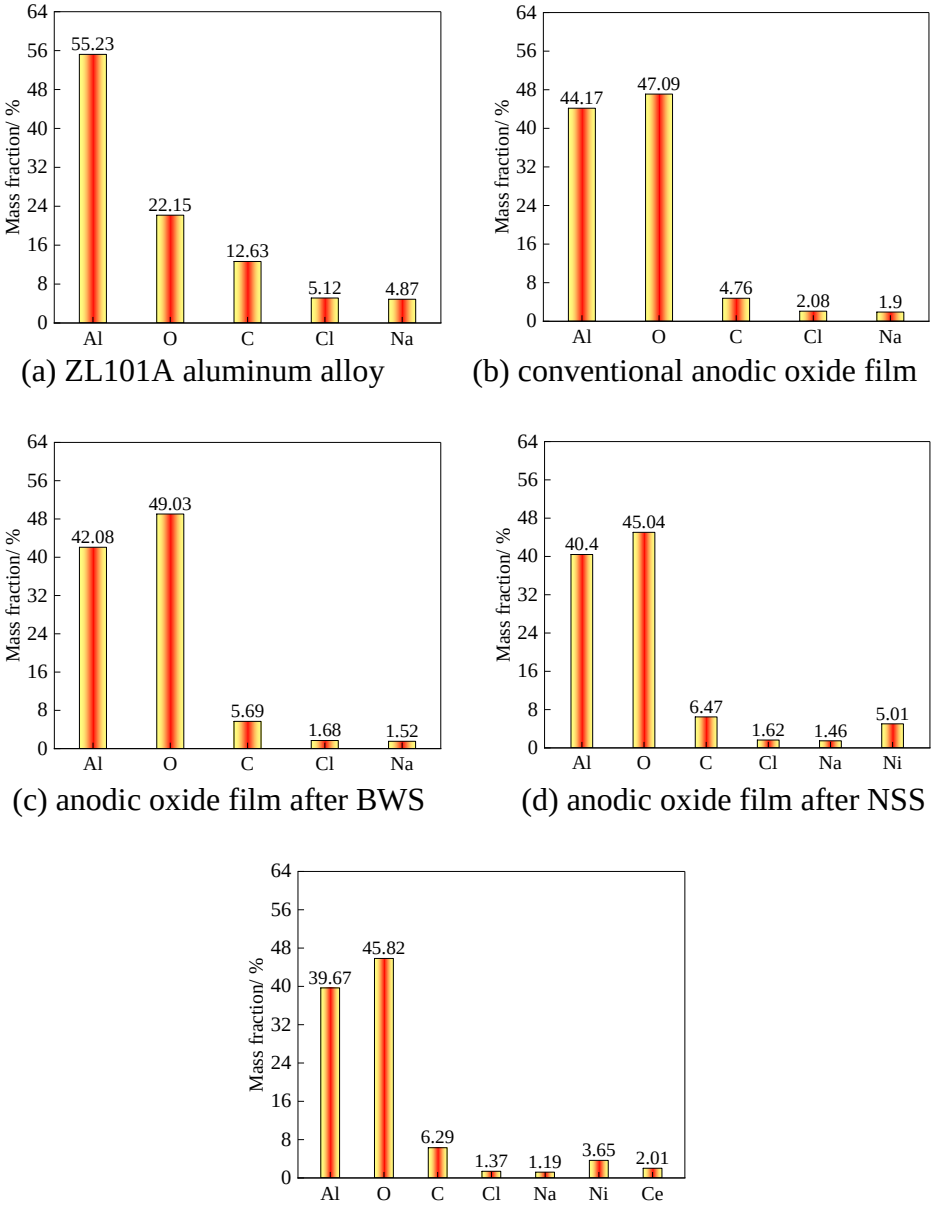

(a) ZL101A aluminum alloy (b) conventional anodic oxide film

(c) anodic oxide film after BWS (d) anodic oxide film after NSS

(e) anodic oxide film after NSS and CSS

Figure 4. Composition of corrosion products on the surface of ZL101A aluminum alloy and different anodic oxide films

3.2.3 Polarization curves analysis

Figure 5 shows polarization curves of ZL101A aluminum alloy and different anodic oxide films immersed in a mixed solution of 3.5% sodium chloride, 2‰ sodium sulfate and 1‰ magnesium chloride for different time. Table 2 shows the electrochemical corrosion parameters related to the polarization curves. The results show that the more positive the corrosion potential is, the lower the corrosion current density is. And the higher the polarization resistance is, the better the corrosion resistance is.

Under the condition of without immersion, it can be seen that the corrosion current density of conventional anodic oxide film and the anodic oxide film after BWS are lower than that of ZL101A

aluminum alloy. Since the corrosion current density is the key factor to determine the corrosion rate, it is determined that the corrosion rate of ZL101A aluminum alloy is reduced by anodic oxidation and sealing treatment, and the corrosion resistance is improved obviously. Among the sealed anodic oxide films, the corrosion current density of the anodic oxide film after synergistic sealing with nickel salt and cerium salt is the lowest, only 4.1×10^{-7} A/cm^2, which is much lower than that of ZL101A aluminum alloy. After immersion in the mixed solution with 3.5% sodium chloride, 2‰ sodium sulfate and 1‰ magnesium chloride for 240 h, the corrosion current density of ZL101A aluminum alloy increases significantly. However, the corrosion current density of conventional anodic oxide film with and without sealing treatment is still lower than that of ZL101A aluminum alloy. With the immersion time extends to 360 h, the corrosion current density of ZL101A aluminum alloy and different anodic oxidation films all show an increasing trend. However, the increase of corrosion current density of the anodic oxidation film after sealing by boiling water, nickel-salt sealing and synergistic sealing with nickel salt and cerium salt is obviously smaller than that of ZL101A aluminum alloy. However, the corrosion current density of anodic oxide film increases very little after synergistic sealing with nickel salt and cerium salt, and remains constant with immersion time extending from 240 h to 360 h. The results show that the corrosion resistance of anodic oxide film decreases gradually and then keep in a stable state after nickel salt sealing and synergistic sealing with nickel salt and cerium salt, which can inhibit the electrochemical corrosion of ZL101A aluminum alloy in a longer period, thus showing excellent corrosion resistance.

Hydrated alumina, nickel hydroxide precipitation and cerium hydroxide precipitation are simultaneously generated during synergistic sealing with nickel salt and cerium salt, which plays a multi-sealing role and better fills the pores and defects of anodic oxide film to improve the compactness and corrosion resistance. Moreover, during the corrosion process, a layer of relatively dense corrosion product film is formed on the surface of anodic oxide film after synergistic sealing with nickel salt and cerium salt, which prevents the penetration of corrosive medium into the depth of anodic oxide film, and also reduces the corrosion rate of anodic oxide film. Dense corrosion products on the surface can inhibit the corrosion process to improve the corrosion resistance [31-32].

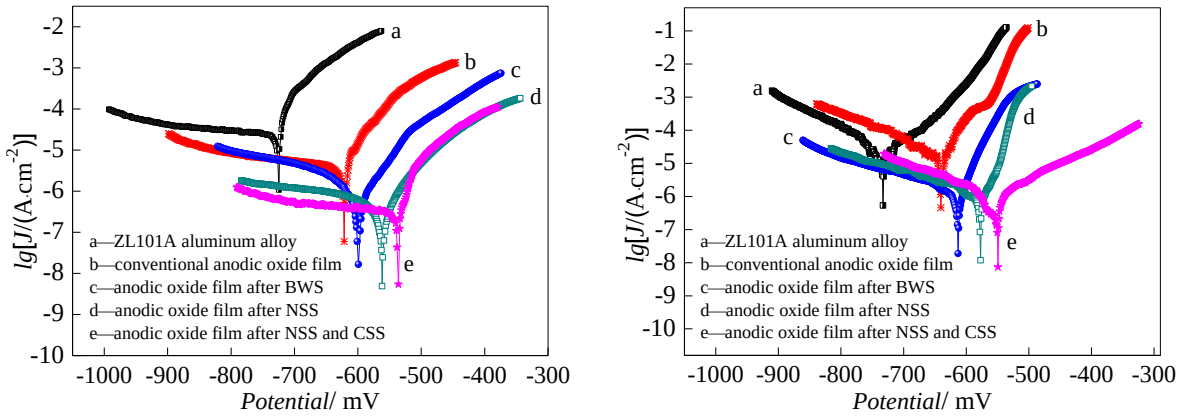

(a) without immersion (b) immersed for 240 h

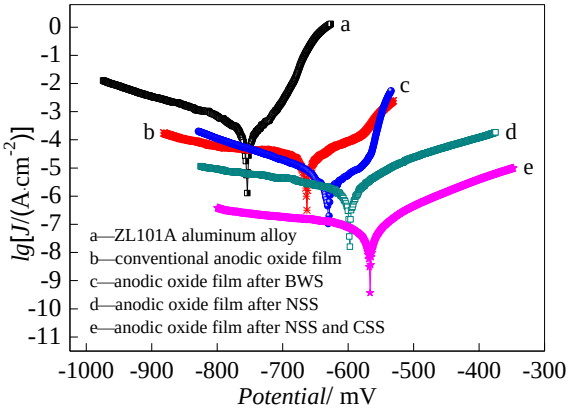

(c) immersed for 360 h

Figure 5. Polarization curves of ZL101A aluminum alloy and different anodic oxide films immersed in a mixed solution of 3.5% sodium chloride, 2‰ sodium sulfate and 1‰ magnesium chloride for different time

Table 2. Electrochemical corrosion parameters related to the polarization curves

Different samples	Corrosion potential/ mV			Corrosion current density/ (A·cm^{-2})		
	without immersion	immersed for 240 h	immersed for 360 h	without immersion	immersed for 240 h	immersed for 360 h
ZL101A aluminum alloy	-716	-733	-754	3.3×10^{-5}	1.4×10^{-4}	2.8×10^{-4}
conventional anodic oxide film	-622	-640	-662	4.9×10^{-6}	1.6×10^{-5}	7.2×10^{-5}
anodic oxide film after BWS	-599	-613	-630	1.3×10^{-6}	5.6×10^{-6}	1.6×10^{-5}
anodic oxide film after NSS	-562	-577	-598	7.2×10^{-7}	1.4×10^{-6}	4.0×10^{-6}
anodic oxide film after NSS and CSS	-537	-550	-566	4.1×10^{-7}	9.0×10^{-7}	1.2×10^{-7}

According to the corrosion current density, the protection efficiency of different anodic oxide films immersed in a mixed solution of 3.5% sodium chloride, 2‰ sodium sulfate and 1‰ magnesium chloride for different time on ZL101A aluminum alloy is obtained. Figure 6 shows that the protection efficiency of conventional anodic oxide film on ZL101A aluminum alloy is about 85.2% without immersion. After boiling water sealing, nickel salt sealing and synergistic sealing with nickel salt and cerium salt, the protection efficiency of anodic oxide film on ZL101A aluminum alloy is increased to 96.1%, 97.8% and 98.7%, respectively. Comparatively, the protection efficiency of the anodic oxide film after NSS and CSS on ZL101A aluminum alloy is the highest.

After immersion a mixed solution of 3.5% sodium chloride, 2‰ sodium sulfate and 1‰ magnesium chloride for 240 h, the protection efficiency of conventional anodic oxide film and the anodic oxide film with different seal treatments are 88.6%, 96.0%, 98.8% and 99.3%, respectively.

With the immersion time extends to 360 h, except for that of the anodic oxide film after synergistic sealing with nickel salt and cerium salt, the protection efficiency of conventional anodic oxide film, the anodic oxide film after boiling water sealing, nickel salt sealing all decreases obviously. Moreover, the protection efficiency of the anodic oxide film on ZL101A aluminum alloy is still the highest after synergistic sealing with nickel salt and cerium salt.

Generally speaking, the higher the protection efficiency, the better the anodic oxide film can resist corrosion and provide good protection for the substrate. Although the reaction products generated during the boiling water sealing and nickel salt sealing can play a sealing role and fill the defects of anodic oxide film to improve its compactness, thereby increasing the corrosion resistance and inhibiting the development of corrosion. However, synergistic sealing with nickel salt and cerium salt generates more reaction products, which play a multiple sealing effect and better improve the compactness of the anodic oxide film. Therefore, the anodic oxide film after synergistic sealing with nickel salt and cerium salt possesses the best corrosion resistance, which plays a good protection effect on ZL101A aluminum alloy to meet high requirements of application in simulated marine atmospheric environment.

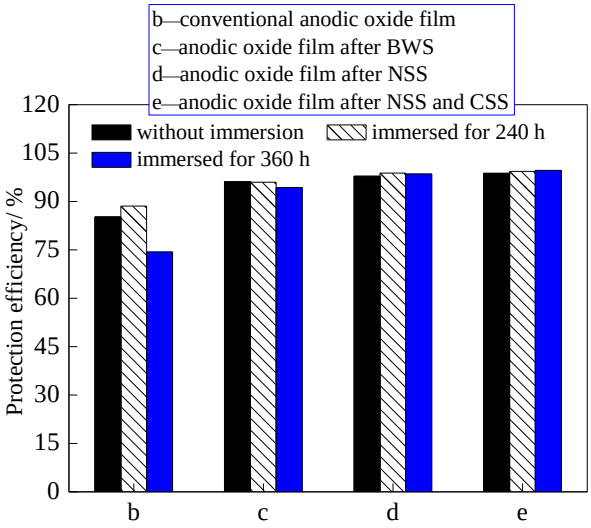

Figure 6. Protection efficiency of different anodic oxide films immersed in a mixed solution of 3.5% sodium chloride, 2‰ sodium sulfate and 1‰ magnesium chloride for different time on ZL101A aluminum alloy

4. CONCLUSIONS

(1) The surface composition of conventional anodic oxide film is Al, O and S elements, which is composed of α-Al_2O_3 and γ-Al_2O_3 phases. The protection efficiency of conventional anodic oxide film on ZL101A aluminum alloy is 85.2%, which can play a certain protective role. After sealing treatment, the surface composition and phase of conventional anode oxide film are changed. The reaction products generated during sealing can fill the defects and pores of the anodic oxide film so as to improve its compactness and corrosion resistance.

(2) Synergistic sealing with nickel salt and cerium salt generates more reaction products, such as hydrated alumina, nickel hydroxide and cerium hydroxide, which play a multiple sealing effect and better improve the compactness of the anodic oxide film. As a result, the anodic oxide film after synergistic sealing with nickel salt and cerium salt possesses the best corrosion resistance, and it protects the ZL101A aluminium alloy well enough to meet the high requirements of application in simulated marine atmospheric environment.

References

1. A. Wang, G. L. Gao, D. Y. Li, D. C. Lu, M. Wang, D. Q. Shi and Z. Y. Xu, *Results Phys.*, 21 (2021) 103822.
2. L. T. Jiang, G. H. Wu, W. S. Yang, Y. G. Zhao and S. S. Liu, *Trans. Nonferrous Met. Soc. China*, 20 (2010) 2124.
3. W. L. Chen, C. Xu, P. L. Pan, X. M. Ruan and H. X. Ji, *Procedia Manuf.*, 50 (2020) 159.
4. J. J. Li, Y. J. Cao, Q. Wang, W. Shang, N. Peng, J. Q. Jiang, L. B. Liang and Y. Q. Wen, *Mater. Today Commun.*, 29 (2021) 102999.
5. M. Mehdizade, A. R. Eivani and M. Soltanieh, *J. Mater. Res. Technol.*, 15 (2021) 68.
6. M. Schneider, U. Gierth and K. Kremmer, *Appl. Surf. Sci.*, 522 (2020) 146438.
7. M. Schneider, T. Liebmann, U. Langklotz and A. Michaelis, *Electrochim. Acta*, 249 (2017) 198.
8. D. Veys-Renaux, N. Chahboun and E. Rocca, *Electrochim. Acta*, 211 (2016) 1056.
9. K. H. Rashid and A. A. Khadom, *Results Phys.*, 4 (2022) 100289.
10. R. X. Wang, L. S. Wang, C. Y. He, M. Lu and L. Sun, *Surf. Coat. Technol.*, 360 (2019) 369.
11. J. Lee, Y. Kim, H. Jang and W. Chung, *Surf. Coat. Technol.*, 243 (2014) 34.
12. M. F. Shaffei, H. S. Hussein, A. M. A. Abouelata, R. M. Osman and M. S. Mohammed, *Cleaner Eng. Technol.*, 4 (2021) 100156.
13. X. W. Yu and C. N. Cao, *Thin Solid Films*, 423 (2003) 252.
14. A. C. Bouali, M. Serdechnova, C. Blawert, J. Tedim, M. G. S. Ferreira and M. L. Zheludkevich, *Appl. Mater. Today*, 21 (2020) 100857.
15. B. Priet, G. Odemer, C. Blanc, K. Grffard and L. Arurault, *Surf. Coat. Technol.*, 307 (2016) 206.
16. M. Sundarajan, M. Devarajan and M. Jaafar, *Mater. Lett.*, 289 (2021) 129425.
17. M. A. Iqbal, H. Asghar and M. Fedel, *J. Alloys Compd.*, 844 (2020) 156112.
18. S. Ono and H. Asoh, *Corros. Sci.*, 181 (2021) 109221.
19. N. P. Hu, X. C. Dong, X. Y. He, J. F. Browning and D. W. Schaefer, *Corros. Sci.*, 97 (2015) 17.
20. S. J. Kim, J. I. Kim and M. Okido, *Korean J. Chem. Eng.*, 21 (2004) 915.
21. D. V. Pronichev, L. M. Gurevich, O. V. Slautin, V. A. Parfenov and V. O. Khalamov, *Metall. Ital.*, 64 (2020) 176.
22. Y. J. Pu, J. J. Hu, T. C. Yao, L. F. Li, J. Zhao and Y. Guo, *J. Mater. Sci. - Mater. Electron.*, 32 (2021) 13708.
23. S. B. Li, D. Ma, Z. Z. Xu, P. Yao, Y. Liu and Y. T. Sun, *Mater. Sci. Rep.*, 24 (2018) 387.
24. D. Liu, G. Y. Wei and P. L. He, *Int. J. Electrochem. Sci.*, 11 (2016) 2097.
25. C. Y. Wang, H. R. Li, P. Zhang and H. Y. Zhao, *J. Mater. Eng. Perform.*, 22 (2013) 624.
26. J. B. Song, J. T. Kim, S. G. Oh, J. S. Shin and J. R. Chun, *Sci. Adv. Mater.*, 7 (2015) 127.
27. H. Jo, S. Lee, D. Kim and J. Lee, *Materials*, 13 (2020) 4904.
28. J. Lee, Y. Kim, J. Kim and W. Chung, *J. Nanoelectron. Optoelectron.*, 9 (2014) 136.
29. A. R. Garcia, E. J. Gonzalez, E. Cano, R. M. Mondragon, J. Genesca and R. Montoya, *Electrochem. Commun.*, 104 (2019) 106485.
30. E. Hakansson, J. Hoffman, P. Predecki and M. Kumosa, *Corros. Sci.*, 114 (2017) 10.
31. H. S. Lee, J. K. Singh and J. H. Park, *Constr. Build. Mater.*, 113 (2016) 905.

32. A. Shamsa, R. Barker, Y. Hua, E. Barmatov, T. L. Hughes and A. Neville, *Corros. Sci.*, 185 (2021) 109423.